FROM THE SOUTHERN OCEAN TO THE NORTH ATLANTIC IN THE EKMAN LAYER?

BY DORON NOF* AND AGATHA M. DE BOER

Contrary to common perceptions, most of the meridional transfer of water from the Southern Ocean to the Northern Hemisphere does not correspond to the Ekman flux in the Southern Ocean.

The idea that the southern winds might be important to the rate of the deep water formation in the North Atlantic was first put forward by Toggweiler and Samuels (1995). They analyzed the results of a global circulation model (GCM) and showed that the rate of North Atlantic Deep Water (NADW) formation increased when the strength of the southern winds was increased. Since a zonal integration of the geostrophic pressure associated with the interior (i.e., the domain below the top Ekman layer and above bottom topography) over the Southern Ocean vanishes, and since there can be no local transformation of Ekman water to deep water, they concluded that the transformation must take place in the North Atlantic via the NADW. In this scenario, the Ekman flux in the Southern Ocean must somehow find its way to the Northern Hemisphere where, through cooling, it sinks to the bottom. We shall show here that, although the mass flux of water crossing the equator is indeed equal to the Ekman flux in the Southern Ocean, the crossing waters do not originate in the southern Ekman layer but rather in the southern *Sverdrup interior*.

AFFILIATIONS: NOF—Department of Oceanography, and The Geophysical Fluid Dynamics Institute, The Florida State University, Tallahassee, Florida; DE BOER—Department of Oceanography, The Florida State University, Tallahassee, Florida
CORRESPONDING AUTHOR: Doron Nof, Department of Oceanography 4320, The Florida State University, Tallahassee, FL 32306-4320
E-mail: nof@ocean.fsu.edu
DOI: 10.1175/BAMS-85-1-79

In final form 13 August 2003

Background. The idea of Ekman to deep water conversion in the northern ocean did not go unchallenged and, using numerical integrations, England and Rahmstorf (1999) argue that most of the Ekman–deep water conversion takes place in the South Atlantic and not the North Atlantic. This has some similarity to the idea presented earlier by Döös and Webb (1994) that the Ekman to deep water conversion takes place in stages rather than one single step (such as the NADW formation). Related attempts to examine the role of the continuous zonal pressure gradient in the open Southern Ocean (or its absence) that should be mentioned here are those of McDermott (1996), Tsujino and Suginohara (1999), and Klinger et al. (2002). We shall argue that the question of what happens to the

Ekman flux in the northern part of the Southern Ocean is not the right question to ask because these waters do not participate in the overturning drama.

The "no-Southern-Ocean–Ekman-flux-across-the-equator" idea presented in this article was already mentioned in passing in Nof (2002 and 2003). Here, we present it in a more explicit manner, and explain it in a way that is more suitable for a broader audience than that which one typically reads in the purely oceanographic literature.

Approach. We shall consider a simple single ocean basin similar to that considered in Nof (2000a, 2003) and focus on the case where all the convection occurs in the Northern Hemisphere (Fig. 1). We shall first present a general derivation of the wind–buoyancy transport formula, assuming that the upper layer is continuously stratified and that there is a level of no motion somewhere between 500 and 1500 m. We shall see later that the same transport formula can be derived even without making the level-of-no-motion approximation. Furthermore, we shall see that, with the Boussinesq approximation, the net meridional transport is determined by the wind regardless of the buoyancy flux. This means that the ocean's temperature and salinity fields will always adjust in such a way that the imposed buoyancy can be accommodated for (regardless of the meridional transport). This is followed by an analytical solution for the width of the trans-hemispheric stream and with numerical simulations. Finally, the results are discussed and summarized.

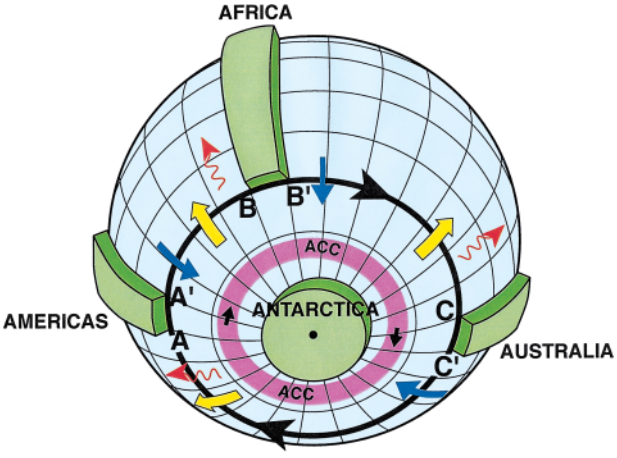

FIG. 1. Schematic diagram of the simplified geography used in Nof (2003). The integration is done along a latitudinal circle passing through the southern tips of the continents (represented by the three peninsulas). The contour is situated inside a latitudinal corridor just *outside* the ACC, where the familiar linearized equations of motion are valid. Red "wiggly" arrow denotes the net meridional mass flux. This net flow is a result of the manner by which the western boundary currents (narrow blue arrows) and the Sverdrup interior (thick yellow arrows) combine.

THE BELT MODEL. Consider again the model shown in Fig. 1, which contains four layers. An upper, continuously stratified, northward-flowing layer contains the Ekman flow, the geostrophic flow underneath, and the western boundary current. It is anywhere from 500 to 1000 m thick where a level of no motion is assumed. The level-of-no-motion assumption coincides with a density surface but its depth varies in the field. Below this level the density is assumed to be constant. The upper-moving layer contains both thermocline and some intermediate water, because some intermediate water is situated above the level of no motion. It is subject to both zonal wind action and heat exchange with the atmosphere. The level-of-no-motion assumption is made merely for convenience and our results can also be obtained without it. In that case the vertical integration is done from the free surface to a fixed level just above the bottom topography.

Underneath the active layer there is a very thick (3000–4000 m) intermediate layer whose speeds [but not necessarily the transport (see, e.g., Gill and Schumann 1979)] are small and negligible. Underneath this thick layer there are two active layers that are not explicitly included in the model and require a meridional wall to lean against. The first is the southward-flowing layer, which carries water such as the NADW; it is ~O(1000 m) thick. The second is a layer containing the northward-flowing Antarctic Water (AABW), whose thickness is ~O(100 m).

Next, a vertically integrated pressure,

$$P^{\star} = \int_{-\zeta}^{\eta} P \, dz,$$

is defined, where ξ is the depth below which the horizontal pressure gradients are small and negligible, η is the free surface vertical displacement (measured positively upward), and P is the deviation of the hydrostatic pressure from the pressure associated with a state of rest. Namely,

$$\partial P/\partial z = -\rho(x,y,z)g,$$

where the density ρ is given by,

$$\rho = \rho_0 + \tilde{\rho}(z) + \rho'(x,y,z),$$

with ρ_0 being the (uniform) density of the lower layer, $\tilde{\rho}(z)$ the density deviation associated with an unforced motionless upper layer, and $\rho'(x,y,z)$ the density deviations associated with the forced stratified upper layer.

Using Leibniz's formula for the differentiation under the integral, one can show that, because $P = 0$ at $z = \eta, -\xi$, vertical integration of the linearized Boussinesq equations from $-\xi$ to η gives,

$$-fV = -\frac{1}{\rho_0}\frac{\partial P^*}{\partial x} + \frac{\tau^x}{\rho_0}, \tag{1}$$

$$fU = -\frac{1}{\rho_0}\frac{\partial P^*}{\partial y} - RV, \tag{2}$$

$$\frac{\partial U}{\partial x} + \frac{\partial V}{\partial y} = 0, \tag{3}$$

where U and V are the vertically integrated transports in the x (eastward) and y (northward) directions, f is the Coriolis parameter (varying linearly with y), τ^x is the stress in the x direction, and R is an interfacial friction coefficient, which, as we shall see, need not be specified for the purpose of our analysis. Friction is only included in the y momentum equation on the grounds that it will be important only within the western boundary current (WBC); that is, the analogous term RU does not appear in (1) because our region of interest is out of the Antarctic Circumpolar Current (ACC) so that U is small. The equations are valid for all latitudes, including the equator. Elimination of the pressure terms between (1) and (2) and consideration of (3) gives,

$$\beta V = -\frac{1}{\rho_0}\frac{\partial \tau^x}{\partial y} - R\frac{\partial V}{\partial x}, \tag{4}$$

which, for the inviscid ocean interior, reduces to the familiar Sverdrup relationship

$$\beta V = -\frac{1}{\rho_0}\frac{\partial \tau^x}{\partial y}. \tag{5}$$

Five comments should be made with regard to (1)–(5).

1) Thermohaline effects enter the equations through the deviation of the hydrostatic pressure from the pressure associated with a state of rest, which is represented in P^*. They are not neglected in the model.
2) Energy is supplied by both the wind and cooling; dissipation occurs through interfacial friction [i.e., the RV term in (2)] within the limits of the WBC system. Interfacial friction is not present in (1) because we assume the RU is small and negligible. Furthermore, since the velocities are small in the ocean interior the frictional term is taken to be negligible there.
3) Relation (1) holds both in the sluggish interior away from the boundaries and in the intense WBC where the flow is geostrophic in the cross-stream direction. Within the WBC the balance is between the Coriolis and pressure terms with the wind stress playing a secondary role. In the interior, on the other hand, the velocities are small and, consequently, all three terms are of the same order.
4) Since *there is a net meridional flow* in our model, the WBC transport is not equal and opposite to that of the Sverdrup interior to its east. Furthermore, since the Sverdrup transport is fixed for a given wind field, it is the WBC that adjusts its transport to accommodate the net meridional transport on the basin.
5) Equations (1)–(5) will be applied to the region shown in Fig. 2 where the induced northward transport is removed via local sinks in the Northern Hemisphere. As is common for many fluid dynamics problems involving point sources and sinks, the equations will only be applied to regions outside the sinks.

A sensible way to proceed with the integration is to follow Nof (2000a,b, 2002) and consider MOCs both in the Atlantic and the Pacific–Indian systems. For this case, integration of (1) from A' to A (i.e., the segment of the contour over the Indian, Pacific, and Atlantic shown in Fig. 1) in a clockwise manner gives

$$f_0 T = \int_{A'}^{A} \frac{\tau^x}{\rho_0} dx. \tag{6}$$

Equation (6) states that the total MOC transport in all oceans combined is equal to the total Ekman transport across the contour $AA'BB'CC'A$. Taking the tips of the peninsulas to have zero width, we find that the transport is roughly 27 Sv (1 Sv $\equiv 10^6$ m^3 s^{-1}; Nof 2003).

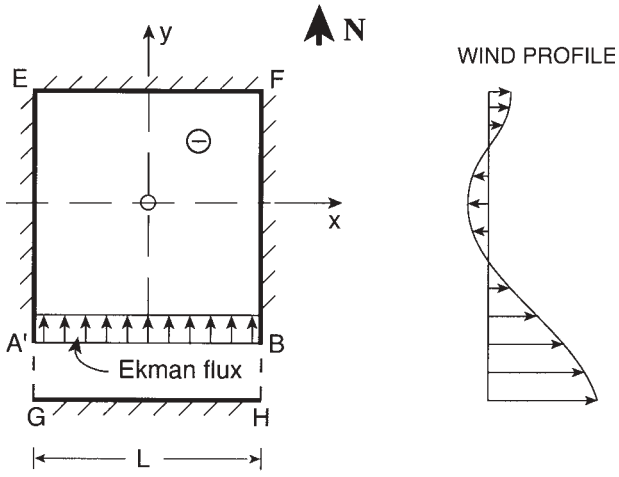

FIG. 2. Top view of the Atlantic model where, as described in Nof (2000a,b), 9 Sv are forced northward. In this scenario, the single basin ocean has one moving layer overlaying a deep stagnant layer. The attached Southern Ocean has periodic boundary conditions at *A′G* and *BH*. These periodic conditions represent the fact that the Southern Ocean encompasses the entire globe, requiring the pressure to be continuous. We shall see that across *AB* the wind pushes northward a flux of $\tau L/f_0$, where τ is the southern wind stress at *A′B*. Buoyancy forces and deep water formation must accommodate this northward flux so that a sink ⊖ must exist in order for a steady state to be reached. Note that the southern winds are considerably stronger than those in the Northern Hemisphere (right). The sink is taken to be a point sink.

Following Nof (2000a,b, 2002) we take the MOC transport in the Atlantic to be 9 Sv and the MOC in the Pacific–Indian system to be the remaining 18 Sv. This division of the 27 Sv among the oceans reflects two processes consistent with each other. The first is that the flow through the Bering Strait is almost zero so that the integral over the Americas and Asia also gives 9 Sv for the Atlantic and 18 Sv for the Pacific (Nof 2000a,b, 2002). The second is that the width of the entrance to the Atlantic from the Southern Ocean (i.e., *A′B*) is about a third of the total contour length (*A′BB′CC′A*), so it is reasonable to take the Atlantic MOC to be also a third of the total MOC. Each of these processes independently leads to the above division of 9 and 18 Sv.

It is a simple matter to show (1) that, with the above division, the pressures along the two southern edges of the Atlantic (*A′G* and *BH*) as well as the pressures along the two southern edges of the combined Pacific and Indian Oceans are periodic. This is because, in each of these basins, the integrated wind stress cancels the integrated transports. The reader can see that this is the case simply by integrating (1) along the southern edge of each of these oceans.

The main point of this article is to show that even though (6) looks like the familiar Ekman transport, it includes the Ekman flow, the geostrophic flow underneath, and the transport of the WBC, because both the equation and the region that we integrated across include those features. We shall see that much of the northward Ekman transport across the Atlantic (Fig. 2) is flushed out of the basin via the recirculating gyres.

Relation (6) gives the combined (wind and thermohaline) transport in terms of the wind field and the geography alone. This means that cooling controls the thermodynamics (i.e., where and how the sinking occurs as well as the total amount of downwelling and upwelling) but does not directly control the net amount of water that enters the ocean from the south. We shall return to this important point momentarily. Equation (6) can only be applied to a latitudinal belt "kissing" the tips of the continents. Away from the tips the ACC is established, and, consequently, form drag, friction, and eddy fluxes are no longer negligible so that an RV term must be added to (1).

We shall see later that, since the interior is in Sverdrup balance, across A′B, the width of the transhemispheric current w is simply determined by the ratio of T to the integrated Sverdrup transport across the basin (times the basin width). One finds

$$w = \beta\tau L/f_0(\partial\tau/\partial y), \qquad (7)$$

where, as before, L is the width of the basin. This condition is valid as long as the total Sverdrup transport across A′B is greater than the transport pushed into the basin, that is, $\partial\tau/\partial y > \beta\tau/f_0$.This is shown in Fig. 3. When $\partial\tau/\partial y$ is small (say, zero), then the entire transhemispheric transport occurs within the western boundary current (Fig. 4). This point will be addressed in detail shortly. It is important to realize that, even though a streamfunction can be obviously defined [because of (3)], such a streamfunction does not have a continuous constant value along the solid boundary *A′EFB* (Fig. 2). This is due to the conversion of upper to lower within the basin, which makes the streamfunction discontinuous along this boundary. Namely, because there is a northward transport in the basin, the streamfunction value on the two meridional boundaries is not the same. To see this more clearly, consider, for example, the situation along the equator. Since there is a meridional transport across it, the value of the streamfunction along the western boundary *A′E* (Fig. 2) is smaller than that on the east-

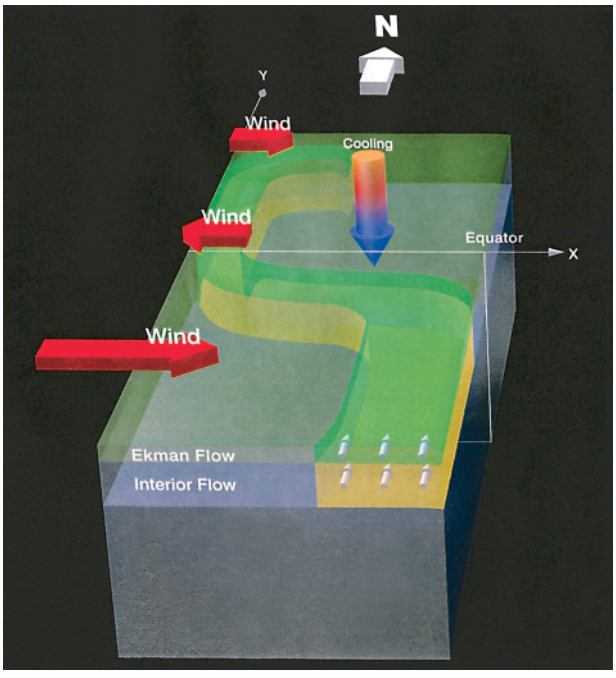

FIG. 3. The 3D path of Southern Ocean water to the north basin in the case where the wind stress curl is either moderate or strong (i.e., $\partial\tau/\partial y \neq 0$). Most of the water that constitutes the "S shaped" path corresponds to interior geostrophic flow along the eastern southern boundary (and not to the southern Ekman flux). Here, both $\tau \neq 0$ and $\partial\tau/\partial y \neq 0$ along the southern edge of the box. The width of the interhemispheric flow (green and yellow) is referred to as "*w*."

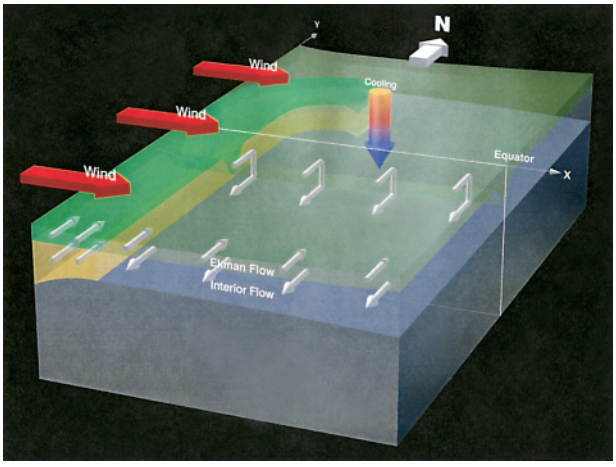

FIG. 4. The 3D path of Southern Hemisphere water to the Northern Hemisphere in the hypothetical case where there is no wind stress curl in the Southern Hemisphere; that is, $\partial\tau/\partial y \equiv 0$ everywhere, but $\tau \neq 0$. Here, there is no net Sverdrup flow; that is, the surface (southern) Ekman flux goes northward all the way to the equator where it sinks and returns southward as an interior geostrophic flow.

ern boundary *FB* (Fig. 2). Although these two boundaries merge to form the northern boundary, the streamfunction cannot merge and, hence, involves a discontinuity. This will become clear later when the numerical simulations will be presented.

NUMERICAL SIMULATIONS. The methodology behind the numerical experiments is the same as that in Nof (2000a, 2002, 2003); that is, we use a nonlinear reduced gravity model with the geometry shown in Fig. 2. The main point to note is that such a model will not reach a steady state without sources and sinks, as it must obey (6) implying that meridional transport must be allowed. The purpose of the numerical simulations is to verify that there are no zonal jets emanating from the tip of the continents and that the zonal flow around Antarctica has no influence on the flow through the section. Such flows (see, e.g., Nof 2000b) could violate our momentum equations.

Instead of verifying the above using very complicated numerical models, we examined numerically the model (Fig. 2) that does not contain very complicated geography. Specifically, we considered a layer-and-a-half application of a "reduced gravity" isopycnic model. This numerical model has no thermodynamics, nor does it have enough layers to correctly represent the ACC. Neither of the two is essential and in order to represent the overturning we introduced two sources in the south and two sinks in the north. The mass flux associated with these sources and sinks is not specified a priori but the sources and sinks are required to handle an identical amount of water.

As in Nof (2000a, 2002, 2003), we let the wind blow, measured the transport established across section *AB,* and then required the sources and sinks to accommodate this measured transport. We continued to do so and continued to adjust the transport until a steady state was ultimately reached. Note that, since our formula gives the transport without giving the complete flow field, it is easiest to start the above runs from a state of rest. Consequently, the initial adjustments that we speak about are not small but they do get smaller and smaller as we approach the predicted transport. The numerical model that we used is the same as that described in Nof (2000a, 2002, 2003) and need not be described again.

Results. Figure 5 shows a typical experiment. In the shown case the numerical transport (nondimensionalized with $g'H^2/2f_{max}$) was 0.87, whereas the analytics gives a somewhat smaller amount of 0.77. Similarly, the theoretical width according to (7) is

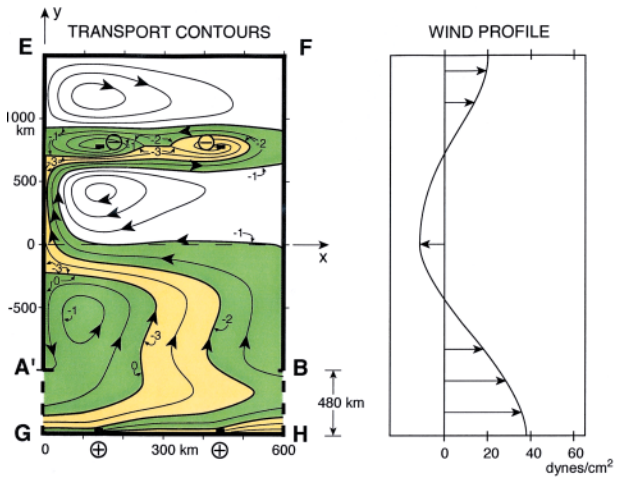

FIG. 5. The nondimensional transport contours for a typical numerical simulation with a rectangular basin subject to periodic boundary conditions at *A′G* and *BH*. The sinks–sources mass flux is not determined a priori. Rather, the model itself determines the mass flux (see text). As mentioned earlier, it is important to realize that, due to the sinks, the streamfunction is not continuous along the solid boundary *A′EFB*. This is perhaps most evident along the equator where the cross-equatorial flow implies that the streamfunction has a value of –1.0 along the eastern boundary and –3.0 along the western boundary. Also, note that the model does not include all the dynamics required for the ACC. Nevertheless, the model does have a tendency to produce such a current. The meridional flow forms an "S shaped" path. For this particular experiment the (nondimensionalized with the basin width) transhemispheric current width according to (9) is 0.59 whereas the displayed numerical value is slightly larger, 0.60. This relatively large ratio (of current width to basin width) is due to the large MOC transport relative to the Sverdrup transport. Parameters: $\Delta x = \Delta y = 15$ km; $AT = 350$ s; $R_d = 20$ km; $g' = 0.015$ m s^{-2}; $H = 600$ m; $\beta = 11.5 \times 10^{-11}$ m^{-1} s^{-1}; $\nu = 16{,}000$ m^2 s^{-1}; $K = 20 \times 10^{-7}$ s^{-1}; $f_{max} = 1.5 \times 10^{-4}$ s^{-1}; wind stress along the southern (northern) boundary is ~ 38 dyn cm^{-2} (2.25 dyn cm^{-2}).

0.59, whereas the simulated value is 0.60. All of our single ocean experiments are essentially a subset of the two basin experiments of Nof (2003) because in his experiments the integrated zonal pressure gradient vanished for each individual basin. Hence, most of them are not reproduced here, and the very good numerical–theoretical agreement found there can also be regarded as the agreement here.

Figure 5 also shows how the MOC crosses the equator. The water enters the southeastern Atlantic through the (linear) interior. It then follows an "S shaped" path and reaches the North Atlantic. One of the most important aspects of Fig. 5 is that it shows very vividly that the waters entering the northern oceans are not Ekman fluxes but Sverdrup interior waters (along the eastern boundaries).

It should be pointed out that it is only the total strength of the MOCs in the Atlantic plus the Pacific and the Indian Oceans that depend on the zonal wind stress integrated along the closed zonal contour encompassing the earth in the Southern Ocean. Hence, the MOC in the Atlantic is not only defined by the wind stress but also by the meridional transport occurring in the Pacific and Indian Oceans.

RELATION OF (6) TO THE ACTUAL EKMAN TRANSPORT. Nof (2003) used National Centers for Environmental Prediction (NCEP) reanalysis data [provided by the National Oceanic and Atmospheric Administration–Cooperative Institute for Research in Environmental Sciences (NOAA–CIRES) Climate Diagnostics Center, Boulder, Colorado, from their Web site at www.cdc.noaa.gov] for annual mean winds (averaged over 40 yr) with a drag coefficient of 1.6×10^{-3} [which is the appropriate coefficient for winds (such as ours) with a speed of less than 6.7 m s^{-1} (see, e.g., Hellerman and Rosenstein 1983)]. With the aid of (6), he found a reasonable net meridional transport of about 27 Sv (over the entire globe).

At first glance, (6) and (7) may give the erroneous impression that the northward Ekman transport across the contour actually represents the MOC, that is, that the fluid that starts in the Southern Ocean and ends up in the Northern Hemisphere coincides with the Ekman transport across the contour shown in Fig. 1. A careful examination shows that this is not the case, as the fluid that constitutes the MOC corresponds to either a fraction of the northward Sverdrup transport or a fraction of the WBC (rather than the Ekman transport). It is merely that the amount of water that is flowing northward is identical to the amount of the Ekman transport. To see this we first note that nowhere in our solution and its derivation has it ever been mathematically stated whether the flow belongs to the WBC, the Sverdrup interior, or the Ekman flow. The only statement that has been made is that it is a combination of the three because (6) corresponds to an integrated quantity. We shall see that how the flow is partitioned between the Sverdrup and the WBC is determined by the *wind stress curl*, which is not even present in (6). A strong or moderate curl implies an eastern current, whereas a weak curl implies a western current.

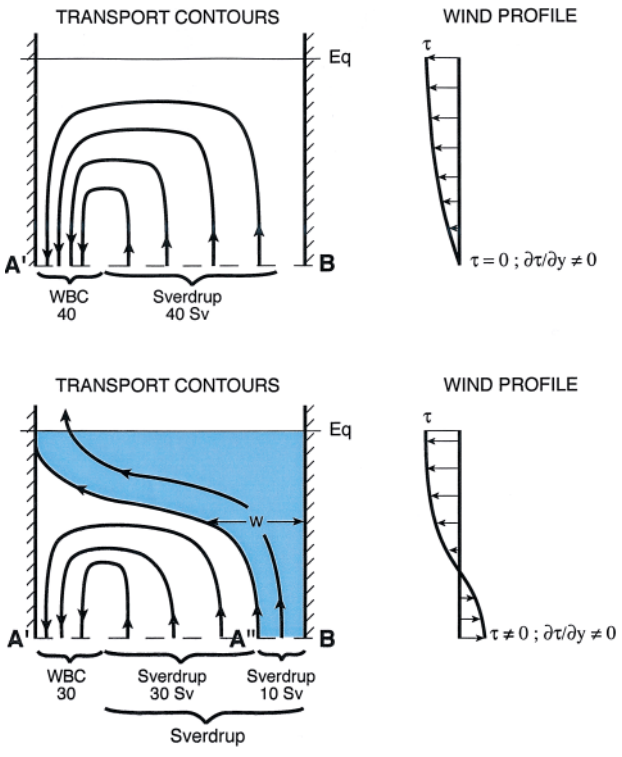

FIG. 6. A cartoon of the South Atlantic flow pattern in the vicinity of the integration contour. (top) The case where (6) gives zero; that is, there is no MOC, and the WBC transport (say, 40 Sv) is equal and opposite to the Sverdrup flow. (bottom) The case where the curl of wind stress is the same as above but the integral of the wind stress across *A′B* is now nonzero (and gives 10 Sv), that is, there is no MOC. Since the Sverdrup balance is fixed by the wind, the only way for the ocean to accommodate the MOC is to weaken the WBC (from 40 to 30 Sv). As a result, the Sverdrup transport (still 40) is now greater than the WBC (30 Sv), and 10 Sv are now flowing northward along the eastern boundary. This 10 Sv ultimately ends up in the Northern Hemisphere. The northward-flowing 10 Sv is also the calculated Ekman transport across *A′B* but corresponds to a different water mass. Most of the Ekman flux across *A′B* (i.e, the Ekman transport associated with *A′A″*) is advected by the fluid below in a circulatory manner and never crosses the equator because it is flushed out of the South Atlantic. Reproduced from Nof (2003).

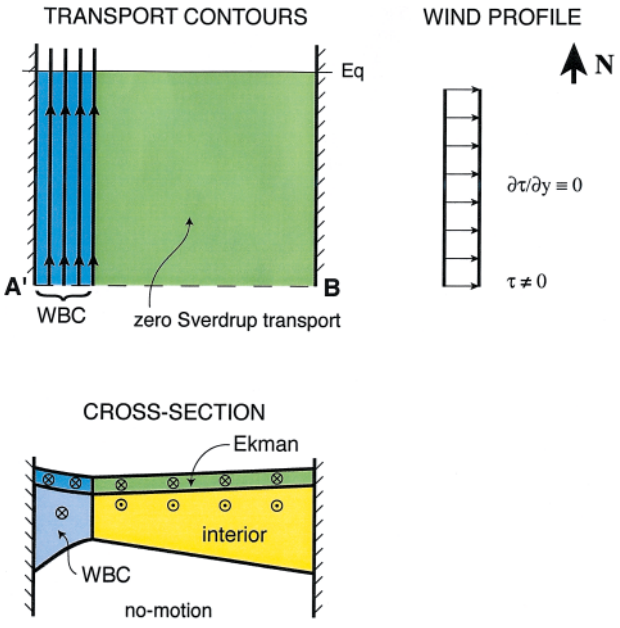

FIG. 7. The hypothetical (special) case of an MOC with no Sverdrup transport (i.e., $\tau \neq 0$, but $\partial\tau/\partial y \equiv 0$ everywhere). Here again, most of the Ekman transport across *A′B* (green) does not participate in the MOC drama even though the WBC transport (6) is the same as the Ekman transport. Since there is no net meridional transport east of the WBC, the northward Ekman transport there (10 Sv shown in green) cannot cross the equator, and hence, it sinks immediately to the south of it. This Ekman transport (green) is compensated for by a southward geostrophic flow immediately underneath (yellow). In turn, this interior flow underneath the Ekman layer (yellow) creates a compensating northward-flowing WBC (light blue), which also carries 10 Sv. Namely, since the geostrophic interior flow must integrate to zero, the northward WBC is established to compensate for the southward geostrophic flow underneath the Ekman layer (yellow). Note that the amount of water associated with the Ekman flux within the WBC region (dark blue) is very small compared to the total Ekman flux (green plus dark blue) because the WBC is much narrower than the basin. Reproduced from Nof (2003).

We shall use two examples to show this. First, we shall look at the general case where the curl is so strong that there is a Sverdrup transport in the interior (Fig. 6) and then we shall look at the special case where the curl is weak, that is, $\partial\tau/\partial y \equiv 0$ everywhere in the basin (Figs. 7 and 4). The second case is highly simplified and is, therefore, easier to understand. Some readers may prefer to look at it first.

Example 1. Consider the southern boundary of the basin and suppose, for a moment, that there is *no* MOC [i.e., the integral of (6) gives zero] so that the WBC transport (say, 40 Sv) is equal to and opposite that of the Sverdrup transport to the east (40 Sv). In this case, $\tau = 0$ along our integration contour but $\partial\tau/\partial y$ is not zero. This is shown in Fig. 6 (top). Next, consider the case where $\partial\tau/\partial y$ remains the same as before, but τ is no longer zero along $A'B$ (Fig. 6, bottom). Suppose further that (6) gives 10 Sv for $A'B$. Since the Sverdrup transport is fixed by the curl of the

wind stress, the only way for the ocean to accommodate this northward transport of 10 Sv (imposed by the nonzero wind stress) is to weaken the WBC (from 40 to 30 Sv). The weakened WBC (Fig. 6, bottom) still forms a recirculating gyre of 30 Sv with the western part of the Sverdrup transport (unshaded region). Its fluid never leaves the Southern Hemisphere because the Sverdrup gyre cannot cross the equator—all the interhemispheric exchange occurs within the frictional WBC. The remaining Sverdrup transport (10 Sv) that does not participate in this recirculating gyre corresponds to the MOC, that is, the fluid ultimately crosses the equator and ends up in the Northern Hemisphere (shaded region). This is the fluid that we are interested in. It is situated next to the eastern boundary and corresponds to 1/4 of the total Sverdrup transport. This MOC transport is of the same amount as that given by the Ekman transport across $A'B$ but it obviously corresponds to a different water mass. Most of the Ekman transport across $A'B$ (the part between A' and A'') is advected in a manner that does not allow it to cross the equator; that is, whatever enters this (unshaded) region is flushed back to the Southern Ocean.

How is this reconciled with the fact that the integral of the geostrophic flow underneath the Ekman layer is zero? Very simply, the fact that there is no net flow in the geostrophic interior does not at all mean that the water that gets into the basin through $A'B$ is the *same* water that gets out via the WBC. All that it means is that there will be *some* water of the same *amount* that leaves through the interior. So, the amount of water going northward through $A''B$ (shaded region in Fig. 6, bottom) is *equal* to the Ekman transport across $A'B$ but constitutes a different water mass than the actual Ekman transport. As we have seen above, most of the entering Ekman transport is flushed back out of the South Atlantic via the WBC.

Example 2. Consider now the special (hypothetical) case of $\partial\tau/\partial y \equiv 0$ everywhere (no Sverdrup transport). Here, the MOC is flowing northward as a WBC with a transport equal to that of the Ekman transport across $A'B$ (Figs. 7 and 4). To see this, note that, since there is no Sverdrup transport east of the WBC, the northward Ekman transport there (10 Sv, shown in green) is compensated for by a southward transport of 10 Sv immediately underneath (yellow). Namely, the Ekman transport (green) proceeds meridionally all the way to the equator, which acts like a wall (for the interior). Immediately south of the equator the Ekman layer thickness goes to infinity implying that the Ekman transport sinks and returns southward as an interior geostrophic flow (yellow).

Since the geostrophic interior transport must integrate across to zero, the southward transport underneath the Ekman layer (yellow) is compensated for by a northward WBC of 10 Sv (light blue). This WBC represents the MOC, which ends up in the Northern Hemisphere. Again, although its transport is equal to that of the Ekman transport, it constitutes an entirely different water mass (i.e., blue rather than green). Note that the Ekman transport within the WBC (dark blue) is negligible compared to the total Ekman flux because the scale of the WBC is much smaller that the basin scale.

This completes the description of our two examples. A final point to be made is that the only time that (6) does coincide with the Ekman transport is when the width of the transhemispheric stream w is identical to the basin width

$$\int_{A'}^{B} \frac{1}{\beta}\frac{\partial \tau}{\partial y}\,dx = \int_{A'}^{B} \frac{\tau}{f_0}\,dx,$$

where A' and B are shown in Fig. 6. Note that, in this integration, the width of the WBC was neglected compared to the basin width L and that, for a wind field that is independent of x, the equation reduces to

$$\frac{1}{\beta}\frac{\partial \tau}{\partial y} = \tau / f_0 .$$

In this hypothetical case the Ekman transport is identical to the Sverdrup transport because there is no flow at all in the geostrophic interior.

CONCLUDING REMARKS. Using earlier theoretical considerations and earlier numerical simulations we illustrate that

1) the upper-layer mass flux of a wind–buoyancy-driven meridional overturning cell originating in the Southern Ocean is given by $\tau L/f\rho$, where τ is the wind stress and L is the width of the basin;
2) this transport is, of course, equal to the Ekman transport into the basin but the actual transhemispheric current constitutes a different water mass. It corresponds to a Sverdrup flow along the eastern boundary (Figs. 3, 5, and 6). Its width is $\beta\tau L/f\,\partial\tau/\partial y$, where $\partial\tau/\partial y$ is the wind stress curl. For the South Atlantic the Sverdrup transport is 30 Sv, whereas the MOC is roughly

10 Sv, implying that 1/3 of the eastern South Atlantic corresponds to the transhemispheric exchange;

3) In the special case of no wind stress curl ($\partial\tau/\partial y \equiv 0$) but finite nonzero stress ($\tau \neq 0$), the entire transhemispheric flow takes place within the western boundary current (Figs. 4 and 7).

On this basis, it is suggested that the commonly used integrations of water properties across a latitudinal belt encompassing the entire globe and passing through the Southern Ocean should be interpreted with much caution. This is due to the fact that the Ekman flux, which is a major component of these integrations, does not participate in the interhemispheric mass-flux drama.

ACKNOWLEDGMENTS. This study was supported by the National Science Foundation Contracts OCE 9911324 and OCE 0241036; National Aeronautics and Space Administration Grants NAG5-7630, NGT5-30164, and NAG5-10860; Office of Naval Research Grant N00014-01-0291; and Binational Science Foundation Grant 96-105. Discussions with G. Weatherly were very useful. Computations were done by S. Van Gorder; Figs. 3 and 7 were prepared by Prem Subrahmanyam.

REFERENCES

Döös, K., and D. J. Webb, 1994: The Deacon cell and other meridional cells of the Southern Ocean. *J. Phys. Oceanogr.,* **24,** 429–442.

England, M. H., and S. Rahmstorf, 1999: Sensitivity of ventilation rates and radiocarbon uptake to subgrid-scale mixing in ocean models. *J. Phys. Oceanogr.,* **29,** 2802–2827.

Gill, A. E., and E. H. Schumann, 1979: Topographically induced changes in the structure of an inertial coastal jet: Application to the Agulhas Current. *J. Phys. Oceanogr.,* **9,** 975–991.

Hellerman, S., and M. Rosenstein, 1983: Normal monthly wind stress over the world ocean with error estimates. *J. Phys. Oceanogr.,* **13,** 1093–1104.

Klinger, B. A., J. P. McCreary, and R. Kleeman, 2002: The relationship between oscillating subtropical wind stress and equatorial temperature. *J. Phys. Oceanogr.,* **32,** 1507–1521.

McDermott, D., 1996: The regulation of Northern Hemisphere overturning by Southern Hemisphere winds. *J. Phys. Oceanogr.,* **26,** 1234–1255.

Nof, D., 2000a: Does the wind control the import and export of the South Atlantic? *J. Phys. Oceanogr.,* **30,** 2650–2667.

——, 2000b: Why much of the circulation in the Atlantic enters the Caribbean Sea and very little of the Pacific circulation enters the Sea of Japan. *Progress in Oceanography,* Vol. 45, Elsevier, 39–67.

——, 2002: Is there a meridional overturning cell in the Pacific and Indian Ocean? *J. Phys. Oceanogr.,* **32,** 1947–1959.

——, 2003: The Southern Ocean's grip on the northward meridional flow. *Progress in Oceanography,* Vol. 56, Elsevier, 223–247.

Toggweiler, J. R., and B. Samuels, 1995: Effect of Drake Passage on the global thermohaline circulation. *Deep-Sea Res.,* **42,** 477–500.

Tsujino, H., and N. Suginohara, 1999: Thermohaline circulation enhanced by wind forcing. *J.Phys. Oceanogr.,* **29,** 1506–1516.

Zalesak, S. T., 1979: Fully multidimensional flux-corrected transport algorithms for fluids. *J. Comput. Phys.,* **31,** 335–362.